An Acad Bras Cienc (2021) 93(1): e20200019 DOI 10.1590/0001-3765202120200019
Anais da Academia Brasileira de Ciências | *Annals of the Brazilian Academy of Sciences*
Printed ISSN 0001-3765 I Online ISSN 1678-2690
www.scielo.br/aabc | www.fb.com/aabcjournal

GEOCIENCES

Lipid-matrix effects on tyrosinase immobilization in Langmuir and Langmuir-Blodgett films

MATHEUS S. PEREIRA, MATEUS D. MAXIMINO, CIBELY S. MARTIN, PEDRO H.B. AOKI, OSVALDO N. OLIVEIRA JR & PRISCILA ALESSIO

Abstract: The immobilization of the enzyme tyrosinase (Tyr) in lipid matrices can be explored to produce biosensors for detecting polyphenols, which is relevant for the food industry. Herein, we shall demonstrate the importance of the lipid composition to immobilize the enzyme tyrosinase in Langmuir-Blodgett (LB) films. Tyr could be incorporated into Langmuir monolayers of arachidic acid (AA), 1,2-dipalmitoyl-sn-glycero-3-phosphocholine (DPPC) and 1,2-dipalmitoyl-sn-glycero-3-phospho-(1'-rac-glycerol) (sodium salt) (DPPG), having as the main effect an expansion in the monolayers. Results from polarization-modulated infrared reflection-absorption spectroscopy (PM-IRRAS) pointed to electrostatic interactions between the charged residues of Try and the lipid headgroups, in addition to changes in the order of lipid chains. The interaction between Tyr and DPPC in Langmuir monolayers can be correlated with the superior performance of DPPC/Tyr LB films used as biosensors to detect catechol by cyclic voltammetry. The molecular-level interactions assessed via PM-IRRAS are therefore believed to drive an immobilization process for Tyr in the lipid LB matrix and may serve as a general criterion to identify matrices that preserve enzyme activity.

Key words: Lipid-matrix, tyrosinase, Langmuir-Blodgett, PM-IRRAS, cyclic voltammetry.

INTRODUCTION

The incorporation of enzymes in solid films using casting, spin-coating, electrodeposition and methods providing organized molecular architectures, e.g., Langmuir-Blodgett (LB) (Blodgett 1935) and layer-by-layer (LbL) (Decher et al. 1992), is useful for various applications, including biosensing (Crespilho et al. 2006, Leontidis 2016, Moriizumi 1988). Of particular relevance is the LB immobilization of proteins in lipid matrices (Carralero Sanz et al. 2005, Vidal et al. 2006), which offer a suitable environment for the proteins to retain their activity (Caseli 2018). A key advantage in this methodology is the control of varied parameters such as pH, lipid composition, subphase composition, transfer speed, numbers of layers, and ultimately control of the molecular architecture. This versatility comes with a price as the successful immobilization depends on a suitable choice of such parameters, especially the lipids that are most effective for immobilizing a given protein. The initial settings to be optimized are those related to the spreading of insoluble amphiphiles at the air/water interface to form Langmuir monolayers, which allow for protein incorporation. Relevant to this purpose are the molecular-level interactions between the protein and the film-forming lipids, normally probed with a combination of thermodynamics and spectroscopy techniques. Protein incorporation, for instance, may expand the lipid monolayer

with shifts in the surface pressure isotherms (Peng et al. 2017), and affect the organization of the tails which is apparent in the stretching bands of alkylene chains (Boisselier et al. 2017) measured with polarization-modulated infrared reflection absorption spectroscopy (PM-IRRAS) (Blaudez et al. 1993). On the other hand, obtaining such molecular-level information is useful not only for determining conditions for protein immobilization but also to correlate the physiological action of the protein since the Langmuir monolayer serves as a simplified model of a cell membrane (Rosilio 2018).

The enzyme tyrosinase (Tyr) has been incorporated in LB matrices and then used as phenol biosensors in standard solutions of the atrazine and diuron herbicides (Vedrine 2003), bisphenol-A (Yin et al. 2010)(Wu et al. 2012), hydrazine (Wang et al. 1995), dichlorvos pesticide (Vidal et al. 2006), and dopamine (Tembe et al. 2008). Phenols could also be detected in more complex samples such as wine samples (Carralero Sanz et al. 2005, Gomes et al. 2004) and wastewaters (Campuzano et al. 2003). Polyphenols are important to their antioxidant capacity with the ability to interact with free radicals, originating from more stable species (Tsao 2010). Their organoleptic characteristics (Apetrei et al. 2011) are relevant in food products, beverages, salts, natural or artificial oils (Balasundram et al. 2006), being partially responsible for the quality and stability of several natural products (Lu et al. 2000). Polyphenols can also be used in the prevention of cancer and treatment of degenerative diseases, such as cardiovascular diseases, anemia, pulmonary diseases, cataracts, immune system decline, and brain dysfunctions (Apetrei et al. 2011, Manach et al. 2005).

In this study, we exploited the possibility of immobilizing Tyr in LB films made with distinct lipids (arachidic acid, 1,2-dipalmitoyl-sn-glycero-3-phospho-1'-rac-glycerol, and 1,2-dipalmitoyl-sn-glycero-3-phosphocholine) from those tried in the literature (Alessio et al. 2010, Pavinatto et al. 2011) to assess the importance of lipid composition. This assessment was carried out by investigating the molecular-level interactions in Langmuir monolayers and in the performance of a biosensor containing Tyr in the lipid matrix in LB films to detect catechol by cyclic voltammetry.

MATERIALS AND METHODS

Reagents

Arachidic acid (AA, 312,53 g mol^{-1}), 1,2-dipalmitoyl-sn-glycero-3-phospho-(1'-rac-glycerol) (DPPG, 744.95 g mol^{-1}) and 1,2-dipalmitoyl-sn-glycero-3-phosphocholine (DPPC, 734,08 g mol^{-1}) were purchased from Avanti Polar Lipids, while tyrosinase (Tyr, from mushroom, activity of 5370 U mg^{-1}) was purchased from Sigma-Aldrich. Phosphate buffered saline (PBS) solution was prepared using NaH_2PO_4 (119.98 g mol^{-1}) and $Na_2HPO_4.2H_2O$ (117,98 g mol^{-1}) from Sigma-Aldrich. NaCl (Sigma Aldrich, 58.44 g mol^{-1}) was used as a supporting electrolyte in electrochemical measurements. To Langmuir films experients, the lipid solutions were prepared in chloroform (Sigma-Aldrich), and PBS prepared with ultrapure water (resistivity of 18.2 MΩ cm). All chemical reagents were used without further purification.

Langmuir and Langmuir–Blodgett (LB) films

Monolayers of AA, DPPG, and DPPC were formed in a KSV 2000 Langmuir trough (KSV Instruments, Finland) equipped with a Wilhelmy plate to measure surface pressure. An aliquot of 50 µL of lipid solution at 0.5 mg mL^{-1} was spread on the PBS (0.1 mol L^{-1}, pH 7.0) subphase, also containing NaCl (0.1 mol L^{-1}). Tyr incorporation was carried out by injection of 50 µL of Tyr (1.74 mg mL^{-1}) solution into the PBS subphase, before the

barrier compression. The kinetics study was performed under the same conditions described above but without the lipid monolayer. All the π-A isotherms from lipids, lipids/Tyr, and containing Tyr in the subphase, were obtained 15 min after spreading (solvent evaporation) at 23ºC with symmetrical compression at 15 mm min^{-1}. The measurements were carried out in triplicate to ensure reproducibility. Polarization-modulation infrared reflection-absorption spectroscopy (PM-IRRAS) measurements from the Langmuir films were performed using a KSV PMI 550 instrument (KSV Instruments Ltd., Helsinki-Finland), with the monolayers previously compressed at 30 mN m^{-1}. The LB lipid films with and without Tyr incorporation were deposited onto transparent indium tin oxide substrates (ITO) at a surface pressure of 30 mN m^{-1}, starting from a submerged position and moving upwards in alternating depositions, lifting the substrate through the air-water interface. They were then placed in a 2% glutaraldehyde solution for 25 min. The dipper speed was varied from 2 $mm.min^{-1}$ to 0.1 $mm.min^{-1}$ to optimize monolayer transfer. LB lipid films were deposited from 1 to a maximum of 5 layers. At the 5^{th} layer, the transfer ratio (RT) decreases to almost zero. Before LB film deposition, ITO substrates were treated in a 70°C solution of H_2O: H_2O_2: NH_4OH in a ratio of 6:1:1 (v/v/v) for 15 min. Then, the substrates were sonicated in isopropyl alcohol and the water for 10 min each. The films were stored in PBS solution at ca. 8ºC.

Electrochemical measurements

Langmuir-Blodgett films of lipids and lipids/Tyr deposited on ITO substrates were evaluated using electrochemical measurements with a potentiostat/galvanostat μ Autolab, type III, in a typical three-electrode cell: ITO substrates covered with LB films were used as working electrodes, Ag/AgCl as a reference electrode, and Pt wire as a counter electrode. The measurements were carried out using 0.01 mol L^{-1} PBS buffer solution with 0.01 mol L^{-1} NaCl as supporting electrolyte in the presence or absence of 120 μmol L^{-1} catechol (Sigma Aldrich, 110,11 g mol^{-1}). The effect of the number of LB layers was evaluated on Tyr/DPPC LB films containing one, three, and five layers. The lipid matrix effect was also investigated using films containing three LB layers of Tyr/DPPC, Tyr/DPPG, and Tyr/AA.

RESULTS AND DISCUSSION

Adsorption kinetics at the air/water interface

Adsorption of Tyr onto a PBS subphase was inferred by monitoring the surface pressure, as shown in Figure 1a. Surface pressure increased to ca. 7.5 mN m^{-1} within 15 min after injection of Tyr, and stabilized at ca. 6.5 mN m^{-1}. This degree of adsorption is higher than observed by Pavinatto et al. 2011 when Tyr diluted in the subphase was incorporated in a matrix of AA:$LuPc_2$ monolayer, where the pressure reached only 1.7 mN m^{-1}. The differences can be ascribed mainly to the ionic force of the subphase (0.28 mol L^{-1} in this work vs. 0.12 mol L^{-1} in Pavinatto et al. 2011). The position and angle of the microsyringe on the subphase to spread the enzyme and concentration (1.71 mg mL^{-1} in this work vs. 1.68 mg mL^{-1} in Pavinatto et al. 2011) may also be a factor, but less significant. A Gibbs monolayer could be formed by compressing the PBS subphase containing Tyr, as shown by the increase in surface pressure in Figure 1b. Adsorption of Tyr at the air/water subphase was favored by the salting-out effect, as the high NaCl concentration in the subphase caused a decrease in Tyr solubility (Campuzano et al. 2003). No phase transition or collapse is noted upon compression, as in most Gibbs monolayers. The x-axis in Figure 1b is given in the percentage of compression area because the number of Tyr molecules at the interface cannot

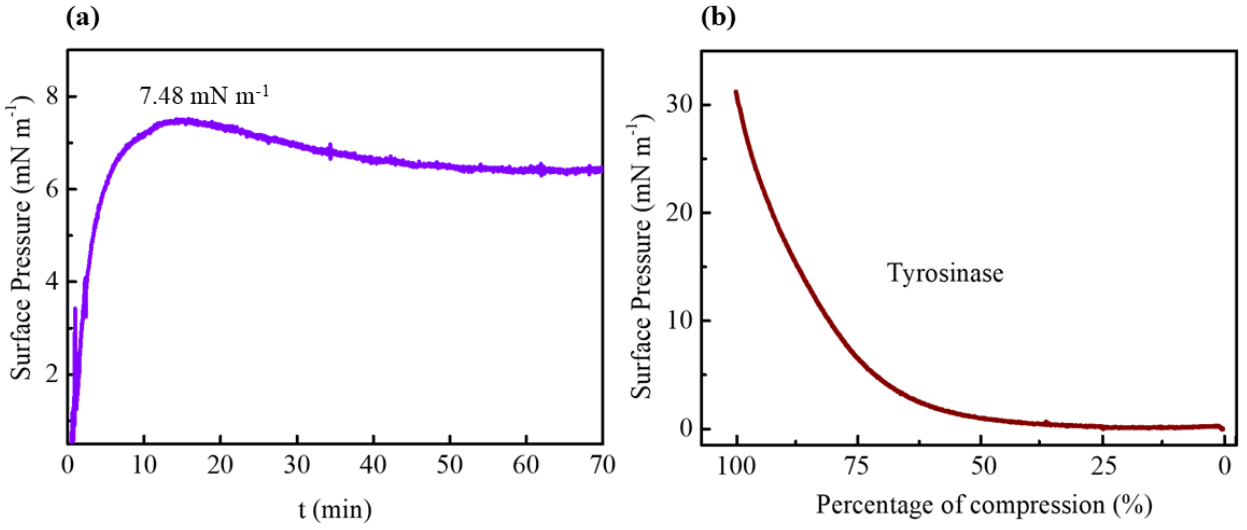

Figure 1. The kinetics of adsorption of 1.74 mg mL^{-1} Tyr injected into the PBS subphase (a). π-A isotherms recorded for pure Tyr at 1.74 mg mL^{-1} on the PBS subphase (b). The x-axis is given in percentage of compression since the amount of Tyr at the interface is unknown.

be estimated owing to this partial solubility. Attempts to transfer the Gibbs Tyr monolayer onto solid substrates failed, as it happened to other monolayers of partially soluble proteins and compounds (Sołoducho et al. 2009, Vidal et al. 2006, Wang et al. 2009).

The π-A isotherms for AA, DPPC, and DPPG monolayers on PBS subphases in Figure 2 are similar to those on ultrapure water, with extrapolated areas to zero pressure being 22 Å^2, 53 Å^2, and 55 Å^2, respectively, close to the reported values in the literature (Gidalevitz et al. 2003, Hoenig et al. 1991, Klopfer et al. 1996). Upon incorporation of Tyr (1.74 mg mL^{-1}) in the subphase, there was a small increase in these areas to 26 Å^2, 60 Å^2, and 64 Å^2, for AA, DPPC, and DPPG, respectively. The most significant effect from Tyr was observed at larger areas per molecule, especially for AA. As Figure 2a shows, the surface pressure started to raise at much larger areas per molecule with Tyr in the subphase, which has also increased the collapse pressure, as a result of the distinct molecular structuring at the air/water interface (Scholl et al. 2015). Tyr is inferred to be incorporated into the lipid monolayer, with penetration in the hydrophobic tail region, as will be confirmed with PM-IRRAS results later on. At pH 7.0, the AA molecules are mostly deprotonated (Pezron et al. 1990), and Tyr is above its isoelectronic point (4.8), and therefore the negative charges can increase repulsion between AA and Tyr. The main effect from Tyr on DPPC and DPPG isotherms is seen in the liquid-expanded to liquid-condensed (LE/LC) phase transition, with a shift to larger areas that may indicate Tyr penetration (Hendrickson et al. 1983). Also worth noting is that the Tyr effect is almost the same for DPPC and DPPG, despite the latter being negatively charged. It seems that electrostatic interaction between the charged groups in Tyr and the phosphate or the choline in DPPC is sufficient for generating an effect that does not differ much from that on DPPG. At pressures above 30 mN m^{-1}, the isotherms in Figures 2b and 2c coincide with those for neat DPPC and DPPG monolayers on PBS subphases, thus pointing to Tyr molecules being expelled from the region of lipids head, possibly forming a sub-surface (Caseli et al. 2012). At 30 mN m^{-1}, corresponding

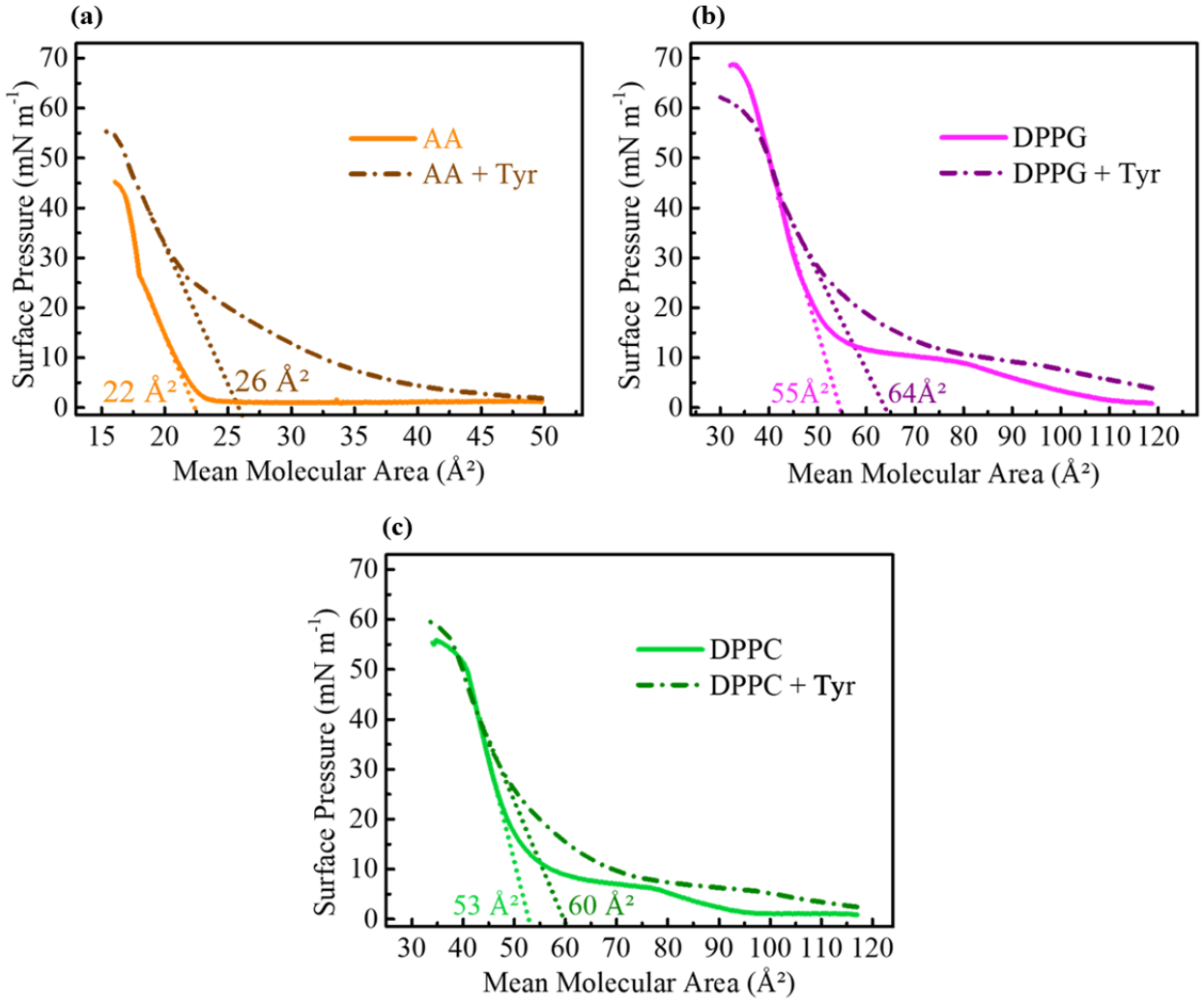

Figure 2. π-A isotherms for Langmuir monolayers of AA (a), DPPG (b), and DPPC (c) at the air/water interface for PBS subphase in absence and presence of Tyr (1.74 mg mL^{-1}).

to the lipid packing of a biomembrane (Marsh 1996), some Tyr molecules remain in all the lipid matrices. Thus, this pressure was used in further experiments. Medina-Plaza et al. 2014 studied the incorporation of Tyr in mixed monolayers of DPPC:$LuPc_2$ transferred to solid films and verified with AFM measurements that adsorption of Ty occurs between the monolayers, similarly to the location of transmembrane proteins in the cell membrane (Medina-Plaza et al. 2014). One may hypothesize that a similar structuring takes place for Tyr adsorbed on the monolayers studied here.

The PM-IRRAS bands expected for the AA headgroups are seen in Figure 3a at 1253 cm^{-1}(O-H bending, δOH), 1469 cm^{-1} (CH_2, δCH_2), and at 1726 and 1753 cm^{-1} assigned to the hydrated and non-hydrated carbonyl bands (νC=O), respectively (Calvez et al. 2001). The incorporation of Tyr did not shift these bands to any significant extent, but other important changes were observed. The downward, broadband assigned to water between ~1550 and 1700 cm^{-1} is considerably decreased, indicating fewer water molecules around AA owing to Tyr molecules in the headgroup region. The well-known bands for

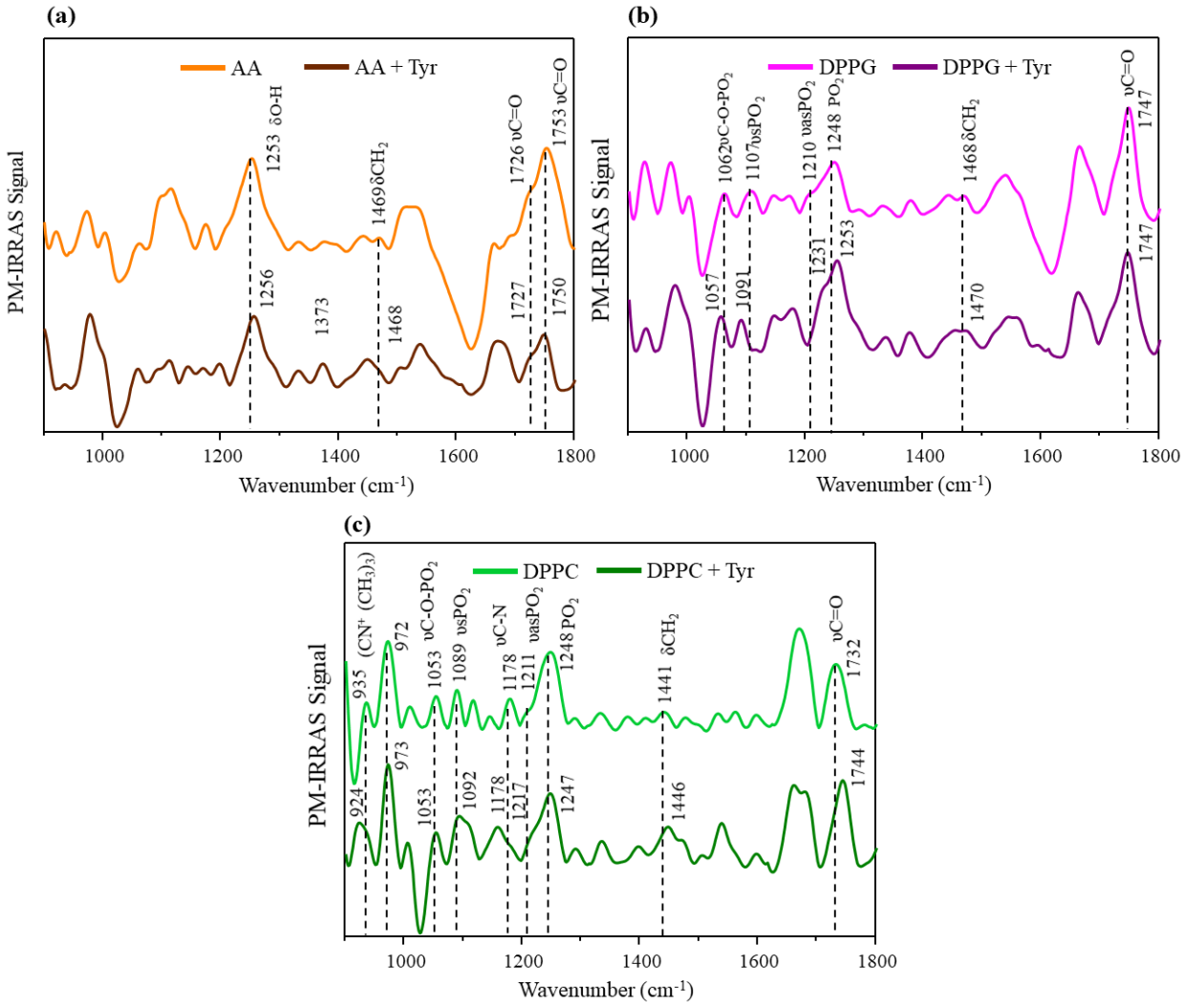

Figure 3. PM-IRRAS spectra at room temperature (~23 °C) and 30 mN/m for neat monolayers and Tyr-containing monolayers on the buffer subphase (1.74 mg mL^{-1}) of AA (a), DPPG (b) and DPPC (c).

DPPG and DPPC monolayers are observed in Figures 3b and 3c, respectively (Ceridório et al. 2016, Geraldo et al. 2013, Maximino et al. 2019). These include the phosphate bands (vC-O-PO_2, v_sPO_2, $v_{as}PO_2$, and monohydrated PO_2), bending of CH_2 (δCH_2), and non-hydrated carbonyl stretching (vC=O), which are present in both lipids. For DPPC, there are also the symmetric and antisymmetric stretching vibrations of choline group ($v_s(CN^+(CH_3)_3)$) at 935 cm^{-1} and v_{as} ($(CN^+(CH_3)_3)$) at 972 cm^{-1}, and the stretching of C-N bonds (vC-N) at 1178 cm^{-1}. Upon incorporating Tyr, the spectrum for DPPG was modified, particularly in the phosphate bands. The vC-O-PO_2 band at 1062 cm^{-1} shifted to 1057 cm^{-1}, the symmetric and antisymmetric stretching bands shifted from 1107 and 1210 cm^{-1} to 1091 and 1231 cm^{-1}, respectively. The monohydrated PO_2 band at 1248 cm^{-1} shifted to 1253 cm^{-1} (Pavinatto et al. 2016). Therefore, Tyr interacted mostly with the negatively charged phosphate group from DPPG, probably via one of its positively charged lateral groups. In DPPC, the phosphate bands were not as affected by Tyr like in the case of DPPG, which

should be expected owing to the zwitterionic group in DPPC headgroups. In contrast, there were significant changes in other headgroup bands: the choline symmetric band shifted from 935 cm^{-1} to 924 cm^{-1}, and the non-hydrated carbonyl band shifted from 1732 cm^{-1} to 1744 cm^{-1}.

Figure 4a shows the PM-IRRAS spectra in 2800 to 3000 cm^{-1} region, corresponding to the alkyl chains. The CH_2 symmetric and antisymmetric stretching bands were observed for all monolayers. There was no significant shift in these bands when Tyr was incorporated into the subphase, but the ratio between intensities of the symmetric and antisymmetric stretching bands was altered, which may be taken as a change in the ordering of the alkyl changes (Goto et al. 2014). Indeed, an increase in this ratio points to disordering in the chains (Ceridório et al. 2016, Levin et al. 1985), while more ordered chains are expected from a decrease in the ratio (Geraldo et al. 2013). As indicated in Figure 4b, Tyr induced disordering in AA chains but ordering in DPPG and DPPC chains. This disordering on AA may be the reason why the band at ca. 2950 cm^{-1} assigned to CH_3 antisymmetric stretching had its intensity decreased considerably with Tyr incorporation.

Overall, Tyr appears to interact more strongly with the headgroups of the lipid monolayers, with considerable effects on the phosphate groups of DPPG. For DPPC there was a smaller effect on the phosphate, but choline and C=O groups were also affected. We may assume that such interactions involved electrostatic attraction between the charged residues of Tyr and the charged moieties in the headgroups.

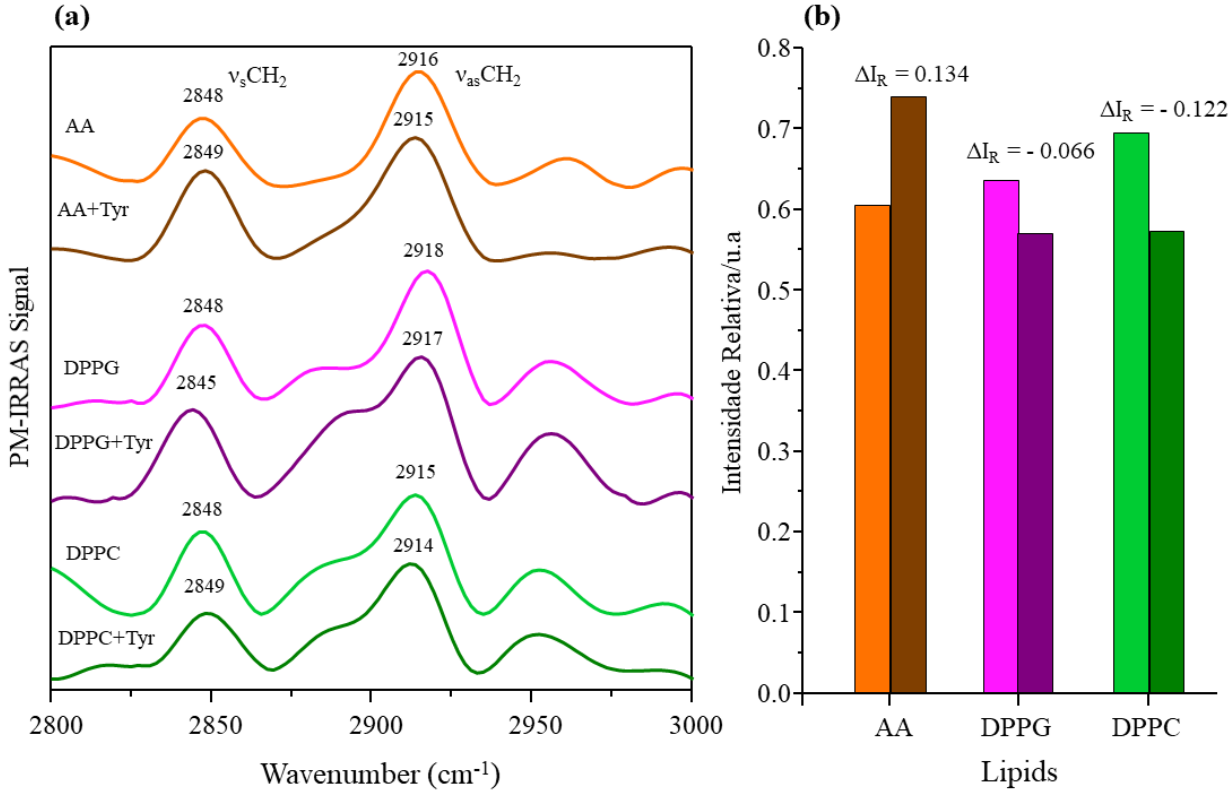

Figure 4. (a) PM-IRRAS spectra for AA, DPPG, and DPPC in the absence and presence of Tyr in buffer subphase at room temperature (23 °C) and the surface pressure of 30 mN/m. (b) Bar graph of the ratio between the relative intensities of the symmetric and antisymmetric stretching bands from CH_2 for each subphase.

Still, we were not able to determine which groups in Tyr took part. In subsidiary experiments, we measured the PM-IRRAS spectrum of a Tyr Gibbs monolayer (Figure S1 - Supplementary Material), which featured several bands that did not appear in the spectra of the Tyr-containing lipid monolayers. To transfer Tyr onto LB films, the results from the surface pressure isotherms and PM-IRRAS spectra indicate increasing suitability according to the order AA < DPPG < DPPC. This inference is based on the stronger ordering effect for the DPPC chains and the possible anchoring onto phosphate, choline, and C=O groups, while for DPPG, such anchoring would be limited to the phosphate groups.

Electrochemical properties towards catechol reduction

Lipids and phospholipids are suitable matrices for enzyme immobilization as they form structures with a high degree of packing, which may preserve the enzyme activity (Apetrei et al. 2012). LB films from lipid matrices are therefore used to achieve organized layers with oriented biological recognition sites. Langmuir films of lipids and lipids/Tyr were deposited as LB films on the ITO surface at 30 mN/m for electrochemical evaluation. Several parameters can be adjusted to optimize performance, the most important of which is the number of layers and the LB film composition. As for the number of layers, we used the most promising lipid

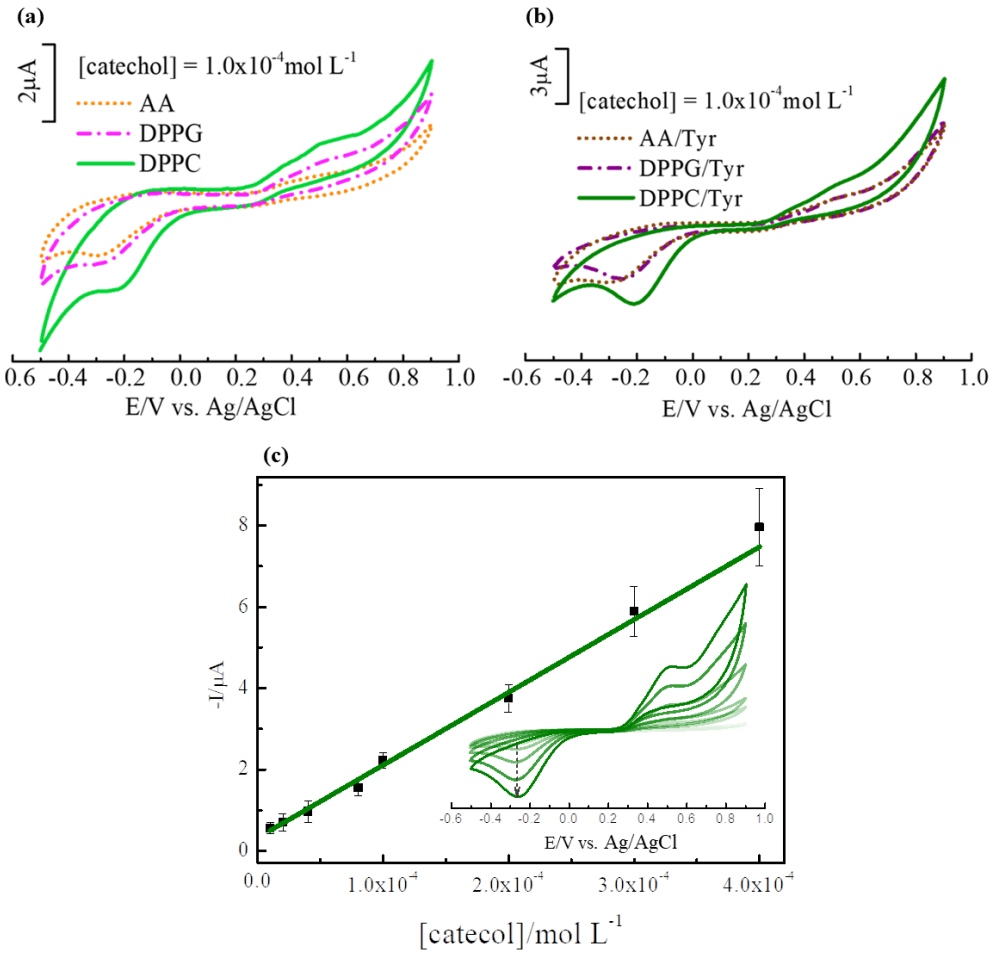

Figure 5. Cyclic voltammograms of AA, DPPG, and DPPC LB films (a); AA/Tyr, DPPG/Tyr, and DPPC/Tyr LB films (b), in the presence of $1.00x10^{-4}$ mol L^{-1} of catechol. v = 25 mV s^{-1}. The analytical curve for the sensor made with DPPC/Tyr LB film to detect catechol from 10^{-5} mol L^{-1} to $4x10^{-4}$ mol L^{-1}. Inset: Cyclic voltammograms with successive additions of catechol (c).

(DPPC) and varied the number from 1 to 5. We found the strongest electroactive response with 3 layers. The voltammograms for these DPPC and Tyr/DPPC LB films are shown in Figure S2 in the Supplementary Material. Hence, 3-layer LB films made with Tyr/DPPG and Tyr/AA were also exposed to a catechol solution. Cyclic voltammograms of AA, DPPG, and DPPC with and without Tyr are shown in Figure 5. Higher currents were measured for DPPC and DPPC/Tyr LB films than for the other lipids under similar conditions. The latter confirms DPPC as the most suitable lipid matrix to produce LB films to exploit Tyr activity. Besides being able to immobilize Tyr, the LB film containing DPPC also exhibited lower electrical resistivity. Thus, the subsequent studies were performed using DPPC/Tyr LB films. Table I lists the potentials and currents in the CVs.DPPC/Tyr films were used for obtaining the analytical curve, which provides quantitative information such as the limit of detection, the limit of quantification, and the range of detection. Figure 5c shows the analytical curve for the film in a buffer for catechol concentrations between 10^{-5} mol L^{-1} and $4x10^{-4}$ mol L^{-1}. From the linear increase in cathodic and anode peak current with concentration, a calibration curve was obtained for the cathodic peak with $Ipa - I_{pc} = 3.2134x10^{-7} + 0.01789$ [catechol]. A limit of detection (LOD) of $7.59x10^{-6}$ mol L^{-1} and limit of quantification (LOQ) of $2.56x10^{-5}$ mol L^{-1} were calculated according to the criterion 3xSD / slope of the straight line, where SD is the standard deviation of the measurements in the supporting electrolyte without catechol (blank). This LOD value is higher than those reported in the literature (see Table II). However, the sensor is still useful for cases of high concentration of polyphenols, especially in food samples where concentrations may be in the range of mg kg^{-1} (Manach et al. 2004). The reason why the sensing performance towards catechol for the DPPC/Tyr LB film is inferior to previous similar works in the literature may be related to the electron mediator employed in ref (Apetrei et al. 2011, Medina-Plaza et al. 2014, Pavinatto et al. 2011).

CONCLUSIONS

The enzyme Tyr can be incorporated into Langmuir monolayers of the three lipids used, namely AA, DPPG, and DPPC, with the main effect of expanding the surface pressure isotherms. From the PM-IRRAS data, we could infer that Tyr interaction is stronger with DPPC, especially via the positively charged group in the zwitterionic headgroup (choline). Also, changes were also noted in the phosphate groups, C=O vibrations, and in the order of hydrophobic chains. This stronger interaction made the DPPC LB film a more suitable matrix to immobilize Tyr and produce a sensor to detect catechol. Indeed, cyclic voltammetry results pointed to higher currents for DPPC/Tyr LB films than for those

Table I. Potentials of oxidation and reduction of catechol.

Modified Electrode	E_{pa} / V	E_{pc} / V
ITO bare	Na.	-0.21
DPPC	0.51	-0.22
DPPC/Tyr	0.51	-0.20
AA/Tyr	0.51	-0.29
DPPG/Tyr	0.51	-0.24

Table II. Comparison of analytical parameters of Tyr biosensors for catechol.

Biosensor	Detection technique	Linear range (μmol L^{-1})	LOD (μmol L^{-1})	Ref.
Tyr–IL–MWCNT–DHP/GCE	LSV	4.9-1100	0.58	(Vicentini et al. 2013)
Tyr–Nafion–MWCNT/GCE	Chronoamperometry	1-23	0.22	(Tsai & Chiu 2007)
Tyr/ZnO/GCE	Chronoamperometry	10-40.000	6	(Chen et al. 2008)
Tyr-ND-PS/GCE	DPV	5-740	0.39	(Camargo et al. 2018)
PANI/Tyr-SWCNTs	Chronoamperometry	0.25-92	0.08	(Wang et al. 2013)
Tyr–CB-f–DHP/GCE	Chronoamperometry	1-20	0.087	(Ibáñez-Redín et al. 2018)
Tyr/AA/$LuPc_2$	CV	4-150	0.58	(Medina-Plaza et al. 2014)
DPPC/Tyr	CV	10-400	7.59	This work

with the other lipids. Our results demonstrate the importance of the lipid composition in the immobilization of enzymes, which is driven by molecular-level interactions with the lipid matrix. The combination of surface pressure isotherms and PM-IRRAS provides precise information of these interactions, and this may be extended to other biomolecules to be immobilized in LB matrices.

Acknowledgments

This work was supported by the Brazilian agencies Conselho Nacional de Desenvolvimento Científico e Tecnológico (CNPq), Fundação de Amparo à Pesquisa do Estado de São Paulo (FAPESP) (2013/14262-7, 2017/15019-0), and Instituto Nacional de Eletrônica Orgânica (INEO).

REFERENCES

ALESSIO P, PAVINATTO FJ, OLIVEIRA JR ON, DE SAJA SAEZ JA, CONSTANTINO CJL & RODRÍGUEZ-MÉNDEZ ML. 2010. Detection of Catechol Using Mixed Langmuir–Blodgett Films of a Phospholipid and Phthalocyanines as Voltammetric Sensors. The Analyst 135(10): 2591.

APETREI C, ALESSIO P, CONSTANTINO CJL, DE SAJA JA, RODRIGUEZ-MENDEZ ML, PAVINATTO FJ, FERNANDES EGR, ZUCOLOTTO V & OLIVEIRA JR ON. 2011. Biomimetic Biosensor Based on Lipidic Layers Containing Tyrosinase and Lutetium Bisphthalocyanine for the Detection of Antioxidants. Biosens Bioelectron 26(5): 2513-2519.

APETREI C, SAJA J, ZURRO J & RODRÍGUEZ-MÉNDEZ ML. 2012. Advantages of the Biomimetic Nanostructured Films as an Immobilization Method vs. the Carbon Paste Classical Method. Catalysts 2(4): 517-531.

BALASUNDRAM N, SUNDRAM K & SAMMAN S. 2006. Phenolic Compounds in Plants and Agri-Industrial by-Products: Antioxidant Activity, Occurrence, and Potential Uses. Food Chem 99(1): 91-203.

BLAUDEZ D, BUFFETEAU T, CORNUT JC, DESBAT B, ESCAFRE N, PEZOLET M & TURLET JM. 1993. Polarization-Modulated FT-IR Spectroscopy of a Spread Monolayer at the Air/Water Interface. Appl Spectrosc 47(7): 869-874.

BLODGETT KB. 1935. Films Built by Depositing Successive Monomolecular Layers on a Solid Surface. J Am Chem Soc 57(6): 1007-1022.

BOISSELIER E, DEMERS E, CANTIN L & SALESSE C. 2017. How to Gather Useful and Valuable Information from Protein Binding Measurements Using Langmuir Lipid Monolayers. Adv Colloid Interface Sci 243: 60-76.

CAMARGO JR, BACCARIN M, RAYMUNDO-PEREIRA PA, CAMPOS AM, OLIVEIRA GG, FATIBELLO-FILHO O, OLIVEIRA JR ON & JANEGITZ BC.

2018. Electrochemical Biosensor Made with Tyrosinase Immobilized in a Matrix of Nanodiamonds and Potato Starch for Detecting Phenolic Compounds. Anal Chim Acta 1034: 137-143.

CAMPUZANO S, SERRA B, PEDRERO M, JAVIE F, DE VILLENA M & PINGARRÓN JM. 2003. Amperometric Flow-Injection Determination of Phenolic Compounds at Self-Assembled Monolayer-Based Tyrosinase Biosensors. Anal Chim Acta 494(1-2): 187-197.

CARRALERO SANZ V, LUZ MENA MA, GONZÁLEZ-CORTÉS A, YÁÑEZ-SEDEÑO P & PINGARRÓN JM. 2005. Development of a Tyrosinase Biosensor Based on Gold Nanoparticles-Modified Glassy Carbon Electrodes. Anal Chim Acta 528(1): 1-8.

CASELI L. 2018. Enzymes Immobilized in Langmuir-Blodgett Films: Why Determining the Surface Properties in Langmuir Monolayer Is Important? An Acad Bras Cienc 90: 631-644.

CASELI L, TIBURCIO VLB, VARGAS FFR, MARANGONI S & SIQUEIRA JR. 2012. Enhanced Architecture of Lipid-Carbon Nanotubes as Langmuir-Blodgett Films to Investigate the Enzyme Activity of Phospholipases from Snake Venom. J Phys Chem B 116(45): 13424-13429.

CERIDÓRIO LF, CASELI L & OLIVEIRA JR ON. 2016. Chondroitin Sulfate Interacts Mainly with Headgroups in Phospholipid Monolayers. Colloids Surf B Biointerfaces 141: 595-601.

CHEN L, GU B, ZHU G, WU Y, LIU S & XU C. 2008. Electron Transfer Properties and Electrocatalytic Behavior of Tyrosinase on ZnO Nanorod. J Electroanal Chem 617(1):7-13.

CRESPILHO FN, ZUCOLOTTO V, OLIVEIRA JR ON & NART FC. 2006. Electrochemistry of Layer-by-Layer Films: A Review. Int J Electrochem Sci 1: 194-214.

DECHER G, HONG JD & SCHMITT J. 1992. Buildup of Ultrathin Multilayer Films by a Self-Assembly Process: III. Consecutively Alternating Adsorption of Anionic and Cationic Polyelectrolytes on Charged Surfaces. Thin Solid Films 210-211: 831-835.

GERALDO VPN, PAVINATTO FJ, NOBRE TM, CASELI L & OLIVEIRA JR ON. 2013. Langmuir Films Containing Ibuprofen and Phospholipids. Chem Phys Lett 559: 99-106.

GIDALEVITZ D, ISHITSUKA Y, MURESAN AS, KONOVALOV O, WARING AJ, LEHRER RI & LEE KYC. 2003. Interaction of Antimicrobial Peptide Protegrin with Biomembranes. Proc Natl Acad Sci 100(11): 6302-6307.

GOMES SASS, NOGUEIRA JMF & REBELO MJF. 2004. An Amperometric Biosensor for Polyphenolic Compounds in Red Wine. Biosens Bioelectron 20(6): 1211-1216.

GOTO TE & CASELI L. 2014. The Interaction of Mefloquine Hydrochloride with Cell Membrane Models at the Air–Water Interface Is Modulated by the Monolayer Lipid Composition. J Colloid Interface Sci 431: 24-30.

HENDRICKSON HS, FAN PC, KAUFMAN DK & KLEINER DE. 1983. The Effect of a Phase Transition on Penetration of Phospholipid Monolayers by Melittin and Glucagon. Arch Biochem Biophys 227(1): 242-247.

HOENIG D & MOEBIUS D. 1991. Direct Visualization of Monolayers at the Air-Water Interface by Brewster Angle Microscopy. J Phys Chem 95(12): 4590-4592.

IBÁÑEZ-REDÍN G, SILVA TA, VICENTINI FC & FATIBELLO-FILHO O. 2018. Effect of Carbon Black Functionalization on the Analytical Performance of a Tyrosinase Biosensor Based on Glassy Carbon Electrode Modified with Dihexadecylphosphate Film. Enzyme Microb Technol 116: 41-47.

KLOPFER KJ & VANDERLICK TK. 1996. Isotherms of Dipalmitoylphosphatidylcholine (DPPC) Monolayers: Features Revealed and Features Obscured. J Colloid Interface Sci 182(1): 220-229.

LE CALVEZ E, BLAUDEZ D, BUFFETEAU T & DESBAT B. 2001. Effect of Cations on the Dissociation of Arachidic Acid Monolayers on Water Studied by Polarization-Modulated Infrared Reflection - Absorption Spectroscopy. Langmuir 17(3): 670-674.

LEONTIDIS E. 2016. Langmuir-Blodgett Films: Sensor and Biomedical Applications and Comparisons with the Layer-by-Layer Method. In Surface Treatments for Biological, Chemical, and Physical Applications. 1st ed., Wiley-VCH Verlag GmbH & Co. KGaA, p. 181-208.

LEVIN IW, THOMPSON TE, BARENHOLZ Y & HUANG C. 1985. Two Types of Hydrocarbon Chain Interdigitation in Sphingomyelin Bilayers. Biochemistry 24(22): 6282-6286.

LU Y & FOO LY. 2000. Antioxidant and Radical Scavenging Activities of Polyphenols from Apple Pomace. Food Chem 68(1): 81-85.

MANACH C, SCALBERT A, MORAND C, RÉMÉSY C & JIMÉNEZ L. 2004. Polyphenols: Food Sources and Bioavailability. Am J Clin Nutr 79(5): 727-747.

MANACH C, WILLIAMSON G, MORAND C, SCALBERT A & RÉMÉSY C. 2005. Bioavailability and Bioefficacy of Polyphenols in Humans. I. Review of 97 Bioavailability Studies. Am J Clin Nutr 81(30): 230-242.

MARSH D. 1996. Lateral Pressure in Membranes. Biochim Biophys Acta 1286(3): 183-223.

MAXIMINO MD, CONSTANTINO CJL, OLIVEIRA JR ON & ALESSIO P. 2019. Applied Surface Science Synergy in the Interaction of Amoxicillin and Methylene Blue with Dipalmitoyl Phosphatidyl Choline (DPPC) Monolayers. Appl Surf Sci 476: 493-500.

MEDINA-PLAZA C, DE SAJA JÁ & RODRIGUEZ-MENDEZ ML. 2014. Bioelectronic Tongue Based on Lipidic Nanostructured Layers Containing Phenol Oxidases and Lutetium Bisphthalocyanine for the Analysis of Grapes. Biosens Bioelectron 57: 276-283.

MORIIZUMI T. 1988. Langmuir-Blodgett Films as Chemical Sensors. Thin Solid Films 160(1–2): 413-429.

PAVINATTO A, DELEZUK JAM, SOUZA AL, PAVINATTO FJ, VOLPATI D, MIRANDA PB, CAMPANA-FILHO SP & OLIVEIRA JR ON. 2016. Experimental Evidence for the Mode of Action Based on Electrostatic and Hydrophobic Forces to Explain Interaction between Chitosans and Phospholipid Langmuir Monolayers. Colloids Surf B Biointerfaces 145: 201-207.

PAVINATTO FJ, FERNANDES EGR, ALESSIO P, CONSTANTINO CJL, DE SAJA JA, ZUCOLOTTO V, APETREI C, OLIVEIRA JR ON & RODRIGUEZ-MENDEZ ML. 2011. Optimized Architecture for Tyrosinase-Containing Langmuir–Blodgett Films to Detect Pyrogallol. J Mater Chem 21(13): 4995.

PENG Y, LING-LING H, YU-ZHI D, YONG-JUAN X, HUA-GANG N, CONG C, XIAO-LIN L & XIAO-JUN H. 2017. Hooking Horseradish Peroxidase by Using the Affinity Langmuir-Blodgett Technique for an Oriented Immobilization. Appl Surf Sci 403: 89-94.

PEZRON E, CLAESSON PM, BERG JM & VOLLHARDT D. 1990. Stability of Arachidic Acid Monolayers on Aqueous Salt Solutions. J Colloid Interface Sci 138(1): 245-254.

ROSILIO V. 2018. How Can Artificial Lipid Models Mimic the Complexity of Molecule–Membrane Interactions? Advances in Biomembranes and Lipid Self-Assembly 27: 107-146.

SCHOLL FA & CASELI L. 2015. Langmuir and Langmuir-Blodgett Films of Lipids and Penicillinase: Studies on Adsorption and Enzymatic Activity. Colloids Surf B Biointerfaces 126: 232-236.

SOŁODUCHO J, CABAJ J & ŚWIST A. 2009. Structure and Sensor Properties of Thin Ordered Solid Films. Sensors 9(10): 7733-7752.

TEMBE S, KUBAL BS, KARVE M & D'SOUZA SF. 2008. Glutaraldehyde Activated Eggshell Membrane for Immobilization of Tyrosinase from Amorphophallus Companulatus: Application in Construction of Electrochemical Biosensor for Dopamine. Anal Chim Acta 612(2): 212-217.

TSAI YC & CHIU CC. 2007. Amperometric Biosensors Based on Multiwalled Carbon Nanotube-Nafion-Tyrosinase Nanobiocomposites for the Determination of Phenolic Compounds. Sens Actuators B Chem 125(1): 10-16.

TSAO R. 2010. Chemistry and Biochemistry of Dietary Polyphenols. Nutrients 2(12): 1231-1246.

VEDRINE C. 2003. Amperometric Tyrosinase Based Biosensor Using an Electrogenerated Polythiophene Film as an Entrapment Support. Talanta 59(3): 535-544.

VICENTINI FC, JANEGITZ BC, BRETT CMA & FATIBELLO-FILHO O. 2013. Tyrosinase Biosensor Based on a Glassy Carbon Electrode Modified with Multi-Walled Carbon Nanotubes and 1-Butyl-3-Methylimidazolium Chloride within a Dihexadecylphosphate Film. Sens Actuators B Chem 188: 1101-1108.

VIDAL JC, ESTEBAN S, GIL J & CASTILLO JR. 2006. A Comparative Study of Immobilization Methods of a Tyrosinase Enzyme on Electrodes and Their Application to the Detection of Dichlorvos Organophosphorus Insecticide. Talanta 68(3): 791-799.

WANG B, ZHENG J, HE Y & SHENG Q. 2013. A Sandwich-Type Phenolic Biosensor Based on Tyrosinase Embedding into Single-Wall Carbon Nanotubes and Polyaniline Nanocomposites. Sens Actuators B Chem 186: 417-422.

WANG F, WU Y, LIU J & YE B. 2009. DNA Langmuir-Blodgett Modified Glassy Carbon Electrode as Voltammetric Sensor for Determinate of Methotrexate. Electrochim Acta 54(5): 1408-1413.

WANG J & CHEN L. 1995. Hydrazine Detection Using a Tyrosinase-Based Inhibition Biosensor. Anal Chem 67(20): 3824-3827.

WU L, DENG D, JIN J, LU X & CHEN J. 2012. "Nanographene-Based Tyrosinase Biosensor for Rapid Detection of Bisphenol A. Biosens Bioelectron 35(1): 193-199.

YIN H, ZHOU Y, XU J, AI S, CUI L & ZHU L. 2010. Amperometric Biosensor Based on Tyrosinase Immobilized onto Multiwalled Carbon Nanotubes-Cobalt Phthalocyanine-Silk Fibroin Film and Its Application to Determine Bisphenol A. Ana Chim Acta 659(1-2): 144-150.

SUPPLEMENTARY MATERIAL

Figures S1 and S2

How to cite
PEREIRA MS, MAXIMINO MD, MARTIN CS, AOKI PHB, OLIVEIRA JR ON & PRISCILA ALESSIO P. 2021. Lipid-matrix effects on tyrosinase immobilization in Langmuir and Langmuir-Blodgett films. An Acad Bras Cienc 93: e20200019. DOI 10.1590/0001-3765202120200019.

Manuscript received on January 6, 2020;
accepted for publication on May 17, 2020

MATHEUS S. PEREIRA[1]
https://orcid.org/0000-0001-6157-8939

MATEUS D. MAXIMINO[1]
https://orcid.org/0000-0002-0724-8717

CIBELY S. MARTIN[1]
https://orcid.org/0000-0001-5634-525X

PEDRO H.B. AOKI[2]
https://orcid.org/0000-0003-4701-6408

OSVALDO N. OLIVEIRA JR[3]
https://orcid.org/0000-0002-5399-5860

PRISCILA ALESSIO[1]
https://orcid.org/0000-0002-1345-0540

[1]Universidade Estadual Paulista/UNESP, Faculdade de Ciências e Tecnologia, Departamento de Física, Rua Roberto Símonsen, 305, Centro Educacional, Caixa Postal 467, 19060-900 Presidente Prudente, SP, Brazil

[2]Universidade Estadual Paulista/UNESP, Faculdade de Ciências e Letras, Departamento de Biotecnologia, Av. Dom Antônio, 2100, Parque Universitário, Caixa Postal 65, 19806-900 Assis, SP, Brazil

[3]Universidade de São Paulo/USP, Instituto de Física de São Carlos, Av. Trabalhador São Carlense, 400, Parque Arnold Schimidt, Caixa Postal 369, 13566-590 São Carlos, SP, Brazil

Correspondence to: **Priscila Alessio**
E-mail: priscila.alessio@unesp.br

Author contributions

Matheus S. Pereira and Mateus D. Maximino: Investigation, Data curation, Writing - Original Draft, Visualization; Cibely S. Martin: Investigation, Methodology, Data curation, Writing - Original Draft, Writing - Review & Editing, Visualization; Pedro H.B. Aoki: Formal analysis, Writing - Original Draft, Writing - Review & Editing, Visualization; Osvaldo N. Oliveira Jr: Formal analysis, Writing - Original Draft, Writing - Review & Editing, Visualization; Priscila Alessio: Conceptualization, Methodology, Formal analysis, Writing - Original Draft, Writing - Review & Editing, Visualization, Supervision, Project administration, Funding acquisition.